Supplementary Materials

Social decisions from description compared to experience rely on different cognitive and neural processes

Supplementary Table S1. BOLD signals comparing description and experience trials.

(A) BOLD signals stronger for description than experience			
Brain region	**Extent**	**x; y; z**	**TFCE T-stat**
Cerebellum; Brain-Stem	2083	-5; -76; -25	4.11
		-5; -94; 7	*3.67*
		-13; -16; -7	*3.64*
		5; -44; -22	*3.53*
		8; -16; -11	*3.50*
		-30; -66; -29	*3.36*
		-53; -59; -14	*3.03*
		8; -79; -43	*2.97*
		25; -24; -4	*2.95*
		13; 7; -4	*2.86*
		-15; 7; 4	*2.77*
		-18; -96; -11	*2.75*
		3; -66; 4	*2.73*
		-18; -44; -25	*2.46*
		15; -26; -29	*2.39*
		-40; -79; -14	*2.22*
		13; -84; 7	*2.19*
Precuneus Cortex; Superior Parietal Lobule; Supramarginal Gyrus, posterior division; Angular Gyrus; Supramarginal Gyrus, anterior division; Postcentral Gyrus	1185	38; -41; 43	4.29
		-10; -59; 58	*3.82*
		10; -61; 68	*3.79*
		-38; -41; 43	*3.68*
		25; -59; 54	*2.90*
		25; -64; 32	*2.69*
		-23; -66; 36	*2.69*
		58; -34; 54	*2.63*
Middle Frontal Gyrus; Superior Frontal Gyrus; Precentral Gyrus	196	-28; 2; 50	4.34
Middle Frontal Gyrus; Superior Frontal Gyrus; Precentral Gyrus	122	28; 7; 50	4.20
Paracingulate Gyrus; Cingulate Gyrus, anterior division; Superior Frontal Gyrus; Juxtapositional Lobule Cortex	112	5; 17; 43	3.93
Inferior Frontal Gyrus, pars opercularis; Precentral Gyrus; Middle Frontal Gyrus	98	-43; 12; 25	3.30
Cerebellum	37	25; -44; -25	2.97
Precentral Gyrus; Inferior Frontal Gyrus, pars opercularis; Middle Frontal Gyrus	29	43; 7; 25	3.42
Frontal Orbital Cortex; Frontal Pole	19	-33; 29; -7	3.19
Paracingulate Gyrus; Superior Frontal Gyrus	15	3; 44; 32	3.67
Frontal Orbital Cortex; Frontal Pole	12	33; 29; -7	3.39
Occipital Fusiform Gyrus	6	-45; -76; -29	2.55
(B) BOLD signals stronger for experience than description			
Precuneous Cortex; Supracalcarine Cortex; Cuneal Cortex; Cingulate Gyrus, posterior division	33	-3; -64; 25	3.89

The table shows the results of two contrasts, BOLD signals stronger for **A)** description than experience and **B)** experience than description, while controlling for prosociality using the z-scored SVO measure. All reported regions are significant at $p < 0.05$ after whole brain FWE correction at the voxel level and a contiguous voxel extent of at least 5 voxels. The FWE correction was based on 5000 permutations of the threshold free cluster enhancement (TFCE) values. The TFCE values and permutation-derived test statistics were calculated using the randomize function implemented in FSL. All coordinates are listed in MNI space and represent the peaks of contiguous groups voxels as well as peaks > 20 mm apart within the same contiguous grouping. For large groupings of contiguous voxels, we list all labels returned by the Harvard-Oxford Cortical- and Subcortical Structural probabilistic atlases when using the autaq command in FSL.

Supplementary Table S2. BOLD signals stronger in description than experience trials for low SVO individuals.

Brain region	Extent	x; y; z	TFCE T-stat
Tempo parietal Junction*; Occipital Pole; Lateral Occipital Cortex, inferior division; Occipital Fusiform Gyrus; Lingual Gyrus; Intracalcarine Cortex; Lateral Occipital Cortex, superior division	1413	23; -91; 4 *40; -59; 25* **46; -58; 25* *35; -41; -29* *30; -79; -14* *40; -56; 0* *28; -36; -11* *15; -69; 43* *5; -91; -7* *0; -71; 0* *0; -66; 25*	5.06 *4.94* *4.92* *4.30* *4.29* *4.09* *3.79* *3.46* *3.46* *3.17*
Cerebellum	191	-33; -49; -29	4.91
Supramarginal Gyrus, anterior division	183	-38; -29; 32	5.17
Cingulate Gyrus, posterior division; Precuneous Cortex	64	-5; -51; 7	3.88
Cerebellum	43	-13; -56; -40	3.91
Postcentral Gyrus; Superior Parietal Lobule; Supramarginal Gyrus, anterior division	31	-33; -39; 65	3.81
Cingulate Gyrus, posterior division; Hippocampus	25	10; -39; 11	4.42
Precuneous Cortex; Lateral Occipital Cortex, superior division; Superior Parietal Lobule	24	5; -59; 58	3.88
Occipital Fusiform Gyrus; Lingual Gyrus	21	-18; -71; -18	3.71
Precuneous Cortex; Postcentral Gyrus; Cingulate Gyrus, posterior division; Precentral Gyrus	11	-8; -44; 50	3.43
Lateral Occipital Cortex, inferior division; Middle Temporal Gyrus, temporooccipital part; Inferior Temporal Gyrus, temporooccipital part; Occipital Fusiform Gyrus	8	-45; -61; -4	3.92
Cerebellum	6	5; -59; -22	3.94
Lingual Gyrus; Occipital Fusiform Gyrus; Intracalcarine Cortex	6	25; -66; 0	3.17
Brain-stem	5	-13; -41; -29	3.90
Cerebellum	5	-18; -66; -29	3.53

The table shows the results of the contrast BOLD signals stronger for description than experience for selfish individuals. The parametric regressor, selfish individuals, was equal to the median split in SVO measure, classifying individuals below median SVO as selfish. All reported regions are significant at $p < 0.05$ after whole brain FWE correction at the voxel level and a contiguous voxel extent of at least 5 voxels. The FWE correction was based on 5000 permutations of the threshold free cluster enhancement (TFCE) values. The TFCE values and permutation-derived test statistics were calculated using the randomize function implemented in FSL. All coordinates are listed in MNI space and represent the peaks of contiguous groups voxels as well as peaks > 20 mm apart within the same contiguous grouping. For large groupings of contiguous voxels, we list all labels returned by the Harvard-Oxford Cortical- and Subcortical Structural probabilistic atlases when using the autaq command in FSL.

Supplementary Table S3. Neural activity associated with HDDM accumulation rates in description trials only.

Brain region	Extent	x; y; z	TFCE T-stat
Inferior Frontal Gyrus, pars opercularis; Precentral Gyrus	1127	-48; 7; 14 -38; -6; -11 -28; -21; 0 -40; -16; 29 -33; 22; 4 -58; 14; -7 -28; -1; 7 -65; -21; 18 -63; -6; 4	5.01 4.80 4.60 3.73 3.56 3.51 3.50 3.31 2.95
Frontal Operculum Cortex; Inferior Frontal Gyrus, pars opercularis; Inferior Frontal Gyrus, pars triangularis; Central Opercular Cortex	292	40; 17; 14	4.72
Precentral Gyrus; Postcentral Gyrus	193	38; -11; 32	5.09
Intracalcarine Cortex; Lingual Gyrus; Precuneous Cortex; Cingulate Gyrus, posterior division	183	-13; -64; 4	4.69
Insular Cortex; Putamen	176	35; 9; -4	5.33
Thalamus	157	-13; -16; 4	4.33
Lingual Gyrus	64	15; -66; -18	4.51
Superior Frontal Gyrus; Juxtapositional Lobule Cortex	50	-13; -4; 61	5.15
Cerebellum	31	-13; -59; -22	3.53
Thalamus	22	-15; -26; 14	3.67
Lingual Gyrus; Temporal Occipital Fusiform Cortex	20	-20; -54; -4	3.71
Cingulate Gyrus, anterior division; Juxtapositional Lobule Cortex	17	10; -4; 36	4.95
Thalamus, Brain-stem	15	13; -29; 0	3.67
Central Opercular Cortex; Frontal Operculum Cortex	8	35; 7; 18	3.97
Intracalcarine Cortex; Lingual Gyrus; Precuneous Cortex	6	18; -61; 4	3.35
Caudate	6	-15; 2; 18	3.50
Caudate, Putamen	5	-18; 14; 4	3.25

This table shows the results of the contrast BOLD signals for description trials. All reported regions are significant at $p < 0.05$ after whole brain FWE correction at the voxel level and a contiguous voxel extent of at least 5 voxels. The FWE correction was based on 5000 permutations of the threshold free cluster enhancement (TFCE) values. The TFCE values and permutation-derived test statistics were calculated using the randomize function implemented in FSL. All coordinates are listed in MNI space and represent the peaks of contiguous groups voxels as well as peaks > 20 mm apart within the same contiguous grouping. For large groupings of contiguous voxels, we list all labels returned by the Harvard-Oxford Cortical- and Subcortical Structural probabilistic atlases when using the autaq command in FSL.

Supplementary Table S4. Neural activity associated with HDDM accumulation rates stronger in description than experience trials.

Region	Extent	x; y; z	TFCE T-stat
Brain-stem	743	5; -21; -29	5.21
Paracingulate Gyrus; Cingulate Gyrus, anterior division	311	5; 24; 40	5.67
Occipital Fusiform Gyrus	134	35; -69; -22	4.69
Cingulate Gyrus, posterior division; Cingulate Gyrus, anterior division	70	-5; -21; 29	5.12
Superior Frontal Gyrus; Middle Frontal Gyrus; Frontal Pole	68	28; 32; 54	3.81
Precuneous Cortex; Supracalcarine Cortex; Cuneal Cortex	64	13; -61; 25	3.74
Cerebellum	60	-25; -56; -25	3.67
Frontal Pole; Middle Frontal Gyrus; Superior Frontal Gyrus	59	28; 42; 32	3.70
Occipital Fusiform Gyrus; Lateral Occipital Cortex, inferior division; Temporal Occipital Fusiform Cortex; Inferior Temporal Gyrus, temporooccipital part	52	-38; -71; -14	4.35
Planum Polare	39	-43; -6; -22	4.51
Intracalcarine Cortex; Lingual Gyrus; Cuneal Cortex; Precuneous Cortex	38	-15; -76; 7	4.49
Cingulate Gyrus, anterior division	34	5; 7; 25	3.27
Occipital Fusiform Gyrus; Lateral Occipital Cortex, inferior division; Lingual Gyrus	31	-10; -86; -25	3.57
Precentral Gyrus; Superior Frontal Gyrus	24	23; -16; 58	4.29
Brain-stem	22	20; -39; -25	3.50
Precuneous Cortex; Cuneal Cortex; Supracalcarine Cortex; Lateral Occipital Cortex, superior division	21	-8; -64; 32	3.41
Cerebellum	16	38; -46; -36	3.66
Cerebellum	16	-25; -44; -25	3.59
Cerebellum	12	0; -79; -25	3.55
Cerebellum	11	45; -76; -40	2.82
Frontal Pole	8	25; 44; 0	4.30
Cingulate Gyrus, posterior division	7	8; -44; 22	3.33
Cingulate Gyrus, posterior division; Lingual Gyrus; Parahippocampal Gyrus, posterior division; Hippocampus; Thalamus	5	-18; -39; -4	2.93

This table shows the results of the contrast BOLD signals stronger for description than experience for HDDM accumulation rates in prosocial individuals. The accumulation rates are mean drift rates reflecting individual's subjective weights for relative payoffs and outcomes, based on Equation 3 in the methods section. The parametric regressor, prosocial individuals, was equal to the median split in SVO measure, classifying individuals above median SVO as prosocial. All reported regions are significant at $p < 0.05$ after whole brain FWE correction at the voxel level and a contiguous voxel extent of at least 5 voxels. The FWE correction was based on 5000 permutations of the threshold free cluster enhancement (TFCE) values. The TFCE values and permutation-derived test statistics were calculated using the randomize function implemented in FSL. All coordinates are listed in MNI space and represent the peaks of contiguous groups voxels as well as peaks > 20 mm apart within the same contiguous grouping. For large groupings of contiguous voxels, we list all labels returned by the Harvard-Oxford Cortical- and Subcortical Structural probabilistic atlases when using the autaq command in FSL.

Supplementary Table S5. Payoff pairs displayed during experimental waves.

Wave	Payoff Combination		Payoff Combination	
	Payoff Business	Payoff Society	Payoff Business	Payoff Society
1	30	80	60	60
1	40	70	70	40
1	50	60	60	50
1	60	80	70	60
1	40	80	70	30
2	60	80	70	60
2	40	80	70	30
2	40	80	60	50
2	60	60	80	30
2	40	70	50	50
2	50	50	70	30
2	50	80	50	50
3	30	70	60	50
3	30	70	70	40
3	60	80	70	60
3	50	80	80	30
3	50	80	70	50
3	50	80	60	40
3	60	80	60	50
4	30	70	60	50
4	30	70	70	40
4	60	80	70	60
4	50	80	80	30
4	50	80	70	50
4	50	80	60	40
4	60	70	50	60
5	30	70	60	50
5	30	70	70	40
5	60	80	70	60
5	50	80	80	30
5	50	80	70	50
5	50	80	60	40
5	60	70	50	60

Participants were sampled in 5 different waves (wave 1-5) using 4 different choice payoff sets (highlighted in grey and white). Differences in payoffs varied for business and society.

Supplementary Table S6. Number of trials completed during the main-task.

Wave	DE trials	EX trials	Overall trials
1	100	100	200
2	130	130	260
3	130	130	260
4	126	105	231
5	61	49	110

Number of description and experience trials participants completed during each wave during the main behavioral task.

Supplementary Table S7. Number of trials completed during the three day training.

Wave	Training day 1	Training day 2	Training day 3	Overall trials
1	200	200	200	600
2	280	280	280	840
3	280	280	280	840
4	280	280	280	840
5	280	280	280	840

Overall number of trials that participants completed during the three-day online training during each wave. Trials for training day one, two and three are detailed during each wave.

Supplementary Results S1: Results for memory mistakes.

Participants accurately reported the values of the self-profit and society benefit in the choices based on experience. Participants knew the values of the business and society payoffs in the choices based on experience. They consistently chose one set of payoffs over another in experience decisions, rather than responding in a random fashion (Supplementary Supplementary Figure S). Furthermore, participants were able to remember and report the payoff outcomes associated with each response to the different stimuli learned during the training sessions after the final choice task. When quantifying memory mistakes as the number of points between the reported and true payoffs, we found that most participants remembered both business and society payoffs within 10 points of the true value (payoffs ranged from 30-80 points in increments of 10; Supplementary Supplementary Figure S). Individuals made smaller memory errors for business than society payoffs (Coef. Est. -0.53; 95% CI: -0.76, -0.28; Supplementary **Error! Not a valid bookmark self-reference.**), for frequently chosen than rarely chosen payoffs (Coef. Est. -1.73; 95% CI: -2.23, -1.27) and for frequently chosen business than frequently chosen society payoffs (Coef. Est. -0.73; 95% CI: -1.31, -0.21). Finally, participants made larger reporting errors for higher payoffs (Coef. Est. 0.38, 95% CI: 0.07, 0.72).

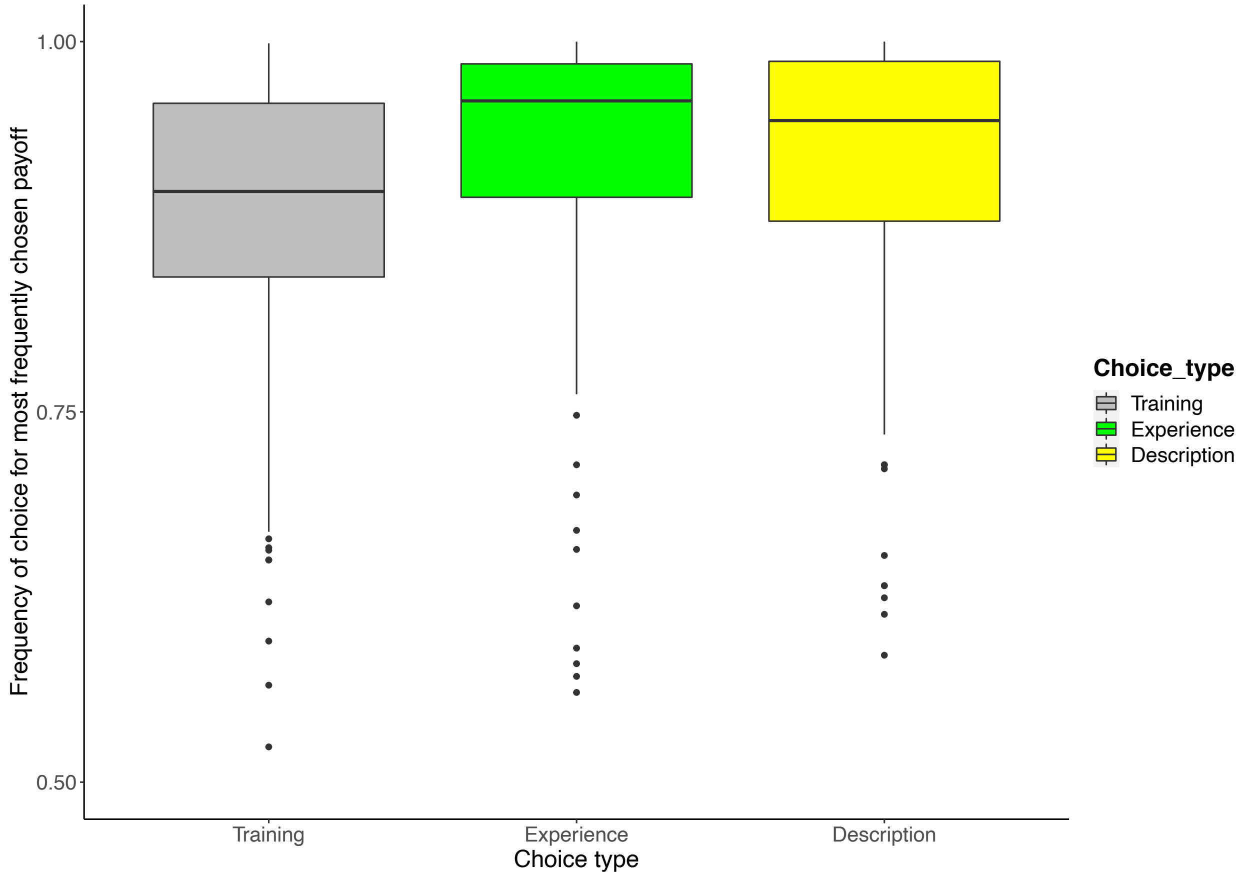

Supplementary Figure S1. Choice consistency for payoffs during the training, experience and description trials.

Individuals consistently chose one set of payoffs over another during the training sessions, as well as in description and experience trials. The frequency of the most frequently chosen payoff was calculated for each individual and respective choice type. The lower and upper hinges of the boxplots indicate the first and third quartiles and the thick line indicates the median. The lower whiskers represent smallest observation less than or equal to lower hinge - 1.5 * interquartile range. The upper whiskers represent largest observation more than or equal to upper hinge + 1.5 * interquartile range. Data points beyond the whiskers are plotted individually (black circles).

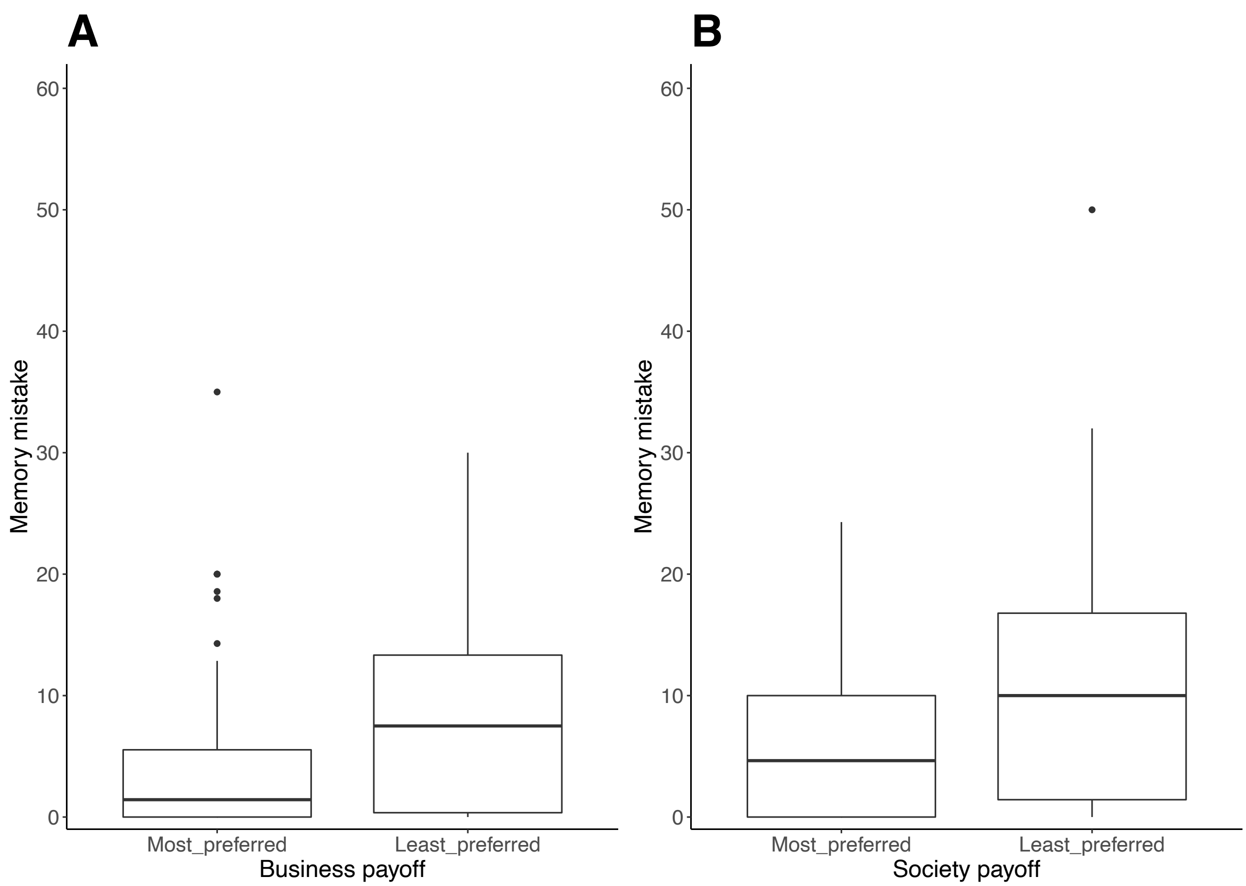

Supplementary Figure S2. Memory mistakes in terms of payoff points.

Memory mistakes were quantified as the absolute value of the number of payoff points between the reported and true payoffs for the stimuli learned during the training sessions. The x-axis divides mistakes according to the most and least preferred **A)** business payoffs and **B)** society payoffs. The lower and upper hinges of the boxplots indicate the first and third quartiles and the thick line indicates the median. The lower whiskers represent smallest observation less than or equal to lower hinge - 1.5 * interquartile range. The upper whiskers represent largest observation more than or equal to upper hinge + 1.5 * interquartile range. Data points beyond the whiskers are plotted individually (black circles).

Supplementary Equation S1: Ordinal Regression for Memory Mistakes.

We computed an ordinal regression to examine memory mistakes as follows (participant-specific slopes and intercepts are omitted for conciseness):

Equation S1: Memory mistake level ~ ß0 + ß1*Business_Payoff * ß2*Frequently_chosen_Payoff + ß3*True_Payoff + ß4*(ß1*Business_Payoff * ß2*Frequently_chosen_Payoff + ß3*True_Payoff | individual) + ε

We used a hierarchical beta regression with grouping effects for each participant (n = 147) to test whether the probability of making memory errors differed for business vs society payoffs (ß1), for payoffs frequently chosen during training (ß2), or as a function of the true payoff value (ß3). Finally, we also tested whether frequently chosen business payoffs were remembered better than frequently chosen society payoffs (ß4). The dependent variable in this regression was the memory mistake level that was quantified as the absolute value of the number of points between the reported and true payoffs with regard to the stimuli learned during the training sessions, ranging on an ordinal scale between 0 and 60 points in steps of 10 (7 levels). The business payoff regressor is a binary vector in which 1 = business payoff and 0 = society payoff. The frequently chosen payoff regressor is a binary vector in which 1 = more frequently chosen payoff and 0 = more rarely chosen payoff. The true payoff is the actual value of the payoff for business or society which the participant had to remember. Values divided by 100 to match the binary regressors. We included participant-specific intercepts and slopes for all regressors. We used an uninformed prior and a probit link function. We ran three independent MCMC chains in STAN and based our inference off of 6000 samples from each chain with a thinning step equal to 1 after a warmup of 6000 samples per chain. We assessed the chains for convergence using the Gelman-Rubin statistic (psrf < 1.05)

Supplementary Table S8. Results of an ordinal Bayesian regression seeking to explain memory mistakes as a function of business payoff, frequently chosen payoff and the true payoff.

	Estimate +/- Est. Error	**95% Credible Interval**
ß1 (Business vs Society)	**-0.53 +/- 0.13**	**[-0.76; -0.28]**
ß2 (Frequently chosen vs rarely chosen)	**-1.73 +/- 0.24**	**[-2.23; -1.27]**
ß3 (True Payoff value)	**0.38 +/- 0.17**	**[0.07; 0.72]**
ß4 (Frequently chosen Business vs Society)	**-0.73 +/- 0.28**	**[-1.31; -0.21]**

This table reports the mean posterior parameter estimates and 95% credible intervals for the population-level parameters from the ordinal regression in Supplementary Equation . The dependent variable, memory error, is an ordered factor with seven levels. Credible intervals different from zero are indicated in bold. The negative coefficients on ß1, ß2, and ß4 indicate that participants made smaller reporting errors for business than society payoffs, frequently chosen than rarely chosen payoffs, and frequently chosen business than frequently chosen society payoffs, respectively. The positive ß3 coefficient indicates that participants made larger reporting errors for higher payoffs.

Supplementary Methods S1: Participant inclusion criteria.

Our inclusion criteria for fMRI were normal or corrected to normal vision, being right-handed, not taking medication for three days prior to the scan session, and no history of psychiatric disease or drug abuse. We discovered that one participant responded to the initial screening incorrectly and proved to be left-handed. His data were already collected when this discovery was made, and thus, we decided to keep him in the sample.

Supplementary Methods S2: Online training for experience trials.

All participants underwent three days of online training to learn the coupling between a specific cue image and payoff pairs before being admitted to the main experiment. Participants learned the outcomes of 5-7 image-payoff pairings during training. The cue images and payoff pairs remained the same for each subject during the online training and the main choice task but were randomized across individuals. Across the different waves of data collection, participants completed an average of 264 (± 33 SD) training trials per day, and 792 (± 107 SD) trials in total over three days (Supplementary Table S7). Each participant was assigned a random fractal image and combination of arrow keys (left or right) for the self-profit maximizing versus societal benefit maximizing outcomes for each unique payoff pair. We also randomized whether the self-profit or the societal benefit was displayed on the left or right side when showing the choice feedback across individuals. During both experience training and the description-experience decision task, hash tags were displayed at either the top/bottom or left/right on the experience cue images. The randomly assigned locations remained the same for each participant throughout the training and the main task. Only participants who completed all of the training on all of the three days were admitted to the main choice task. Note, for 4 of the 147 participants the data from the first training session were not fully recorded due to server errors, however all data from the final choice session was available for all 147 participants. At the end of the three days of online training, participants were paid the average of five trials that were randomly selected from the full set of training trials completed across all three days and one of their choices from the prosociality measure described in the next sub-section.

Supplementary Methods S3: Demographic questions.

What is your age? (Please enter a number)

What is your gender? (Please enter text)

What is your nationality? (Please enter text)

What is your mother tongue? (Please enter text)

How many people live in your hometown? (By 'hometown' we mean the city, town or village where you have spent the majority of your life so far. Please enter text)

What is your marital status? (Please enter text)

Which of the following applies to your present situation? (Please choose)

- In School
- In University
- Employed
- Unemployed
- Stay-At-Home Husband Or Wife
- In Military/Civil/Volunteer Service
- In Retraining
- Other

Which of the following is the highest education level that you have attained?

- High School
- Technical/Vocational School
- Apprenticeship
- Bachelor's
- Master's
- Advanced Professional Degree
- PhD
- Other

If you studied or are studying at university, what is your major? (Please enter text)

Which of the following describes your employment status? (Please choose)

- Student
- Not Working
- Unemployed But Looking For Work

- Less Than 15 Hours Per Week
- 15-34 Hours Per Week
- 35 Hours Per Week Or More
- In Training Or Apprenticeship
- On Temporary Leave
- Other

How wealthy would you say your family is compared to the other families in your home country?

- A Lot Less Wealthy
- Less Wealthy
- Average
- More Wealthy
- A Lot More Wealthy

Supplementary Methods S4: Statistical analyses.

All behavioral data were analyzed using either the Matlab (Release 2016a, version 9.0.0.341360, The MathWorks Inc., 1984, RRID:SCR_001622) or R (Version 3.5.1, R Core Team, 2018, RRID:SCR_001905) statistical software packages.

Supplementary Methods S5: fMRI task timing, data acquisition and preprocessing.

fMRI task timing. Choice screens lasted 3.5 seconds and were presented with a jittered inter-trial interval of 1–8 seconds. The condition (experience, description) remained constant in blocks of 2-10 trials with a 1-8 second jitter between blocks. The block order was randomized across participants.

fMRI data acquisition. All the imaging was conducted at the Laboratory for Social and Neural Systems Research at the University Hospital Zurich using the Philips Achieva 3T whole-body scanner with eight-channel sensitivity encoding head coil. Stimuli were presented using the Psychophysics Toolbox Software (Psychtoolbox 3.0[1], RRID:SCR_002881) with the task projected to mirror the head coil. Images were gradient echo T2*-weighted echo-planar images (EPIs) with blood-oxygen-level-dependent (BOLD) contrast (37 slices per volume, Field of View 200 x 132.6 x 200 mm, slice thickness 3 mm, 0.6 mm gap, in-plane resolution 2.5*2.5 mm, matrix 80*80, repetition time 2344 ms, echo time 30 ms, flip angle 77°) and a SENSE reduction of factor of 1.5. Volumes were acquired in transverse orientation at a -20° tilt to the anterior commissure-posterior commissure line. We collected 500 volumes in ascending order during each of the three experimental runs, together with five “dummy” volumes at the start and end of each run. A T1-weighted turbo field echo structural image was acquired in sagittal orientation for each participant at the end of the scanning session with the same angulation as applied to the functional scans (181 slices, Field of View 256 x 256 x 181 mm, slice thickness 1 mm, no gap, in-plane resolution 1*1 mm, matrix 256*256, repetition time 8.3 ms, echo time 3.9 ms, flip angle 8°). To measure the homogeneity of the magnetic field we collected B0/B1 maps before the first and second runs and before acquiring the structural scan (short echo time = 4.3 ms, long echo time = 7.4 ms). We measured breathing frequency and took an electrocardiogram using the scanner's in-built system in order to correct for physiological noise.

fMRI preprocessing. The statistical parametric mapping software was used for realignment and unwarping functional data (SPM12, Revision nr. 6225, Wellcome Trust Centre for Neuroimaging, 1991, RRID:SCR_007037). Segmentation was implemented with the corresponding T1-weighted high-resolution structural image. Normalization was achieved using the mean EPI template, and images were smoothed using a Gaussian kernel (4 mm full width at half maximum). To decrease physiological noise in the BOLD signal we used the PhysIO toolbox RETROICOR to model respiration and heartbeat[2,3].

Supplementary References

1. Brainard, D. H. & Vision, S. The psychophysics toolbox. *Spatial Vision* **10**, 433–436 (1997).
2. Glover, G. H., Li, T.-Q. & Ress, D. Image-based method for retrospective correction of physiological motion effects in fMRI: RETROICOR. *Magnetic Resonance in Medicine: An Official Journal of the International Society for Magnetic Resonance in Medicine* **44**, 162–167 (2000).
3. Kasper, L. *et al.* Cardiac artefact correction for human brainstem fMRI at 7T. *Neuroimage* **47**, S100 (2009).